103 Radar simulation studies for hydrometeor classification from range profile of polarimetric radar signatures

Takahisa Kobayashi[1,2] , Mistuharu Nomura[1] ,Soichiro Sugimoto[1],Ahoro Adachi[2],
Nobuhiro Nagumo[2] and Hiromaru Hirakuchi[1].
[1] Central Research Institute of Electric Power Industry,1, Abiko,Chiba,Japan,270-1194
[2] Meteorological Research Institute, Tsukuba, Ibaraki, Japan, 305-0035

1. INTRODUCTION

Needless to say, classification of hydrometeors is critical for accurate estimate of precipitation from radar observations because the radar algorithms for estimate are different for type of precipitation. In addition, hydrometeor classification is necessary to prevent disasters caused by accretion of snow on the electric power line, which does not occur in dry snow but occurs in wet snow conditions.

Many hydrometeor classification methods for dual-polarization radars have been developed (eg. Kouketsu et al., 2015, Chandrasekar, et. al., 2013). Most methods use the polarimetric radar signatures such as reflectivity (Ze), differential reflectivity (Zdr), specific differential phase (Kdp), and the correlation coefficient between horizontal and vertical Ze (ρ_{HV}) measured at each radar resolution volume. These parameters often have similar values for different types of precipitation and it is needed to identify the type of precipitation by combining above signatures.

For reflectivity-based rainfall rate estimate, the specific attenuation is an amount to be removed from radar received signals. Many extensive studies have, therefore, focused on the attenuation correction. Attenuation, however, is relatively insensitive to the drop size distribution (DSD) and is closely related to rainfall rate. Therefore, attenuation-based methods for rainfall rate estimate have been developed (Matrosov, 2005, Ryzhkov, et al., 2014). The specific attenuation also depends on the type of precipitation. The attenuation of dry snow is generally small at most radar frequencies. While for rain, large attenuations appear. It has also been reported that melting hails have very large attenuation (Thurai et al., 2015). Larger specific attenuation of the radio wave, in general, appears for higher radar frequencies and can be used for hydrometeor classification as well as rainfall estimate in particular for radars.

There are no straightforward methods for accurate estimate of attenuation. Most methods to estimate attenuation utilize redundancy relations among radar observables. The specific attenuation (A) can be estimated if A is related to the true radar reflectivity factor (Ze^t) by a power law (Hitshchfeld and Bordan,1954). This method was modified by using path-integrated attenuation (PIA) which was used in rainfall rate estimate algorithm in the radar equipped on the Tropical Rainfall Measuring Mission (TRMM) (Meneghini and Nakamura, 1990, Iguchi and Meneneghini, 1994). This method was further modified for the dual frequency space-borne radar (DPR) onboard the Global Precipitation Mission (GPM).

For dual-polarization radars, a linear relationship between the path integrated attenuation (PIA) and the differential phase (Φdp) has been used to estimate attenuation (Bringi et al., 1990, Ryzhkov, et. A., 2014). The

* *Corresponding Author address*: Takahisa. Kobayashi, Central Research Institute of Power Industry, 1646, Abiko, Chiba, 270-1194, Japan
e-mail : kobay@mri-jma.go.jp

redundancy has been also used for attenuation correction (Adachi et al., 2015). These methods are useful, however, the coefficients in the relationships between Φdp and A significantly differ, depending on particle size distribution, precipitation type, and temperature.

To avoid the variation of the coefficients, Kobayashi et al. (2015) have developed a method by using changing tendency of the radar variables in the radar propagation path instead of the variables at each radar resolution volume. The method estimates radar range variations of the relative values of attenuation from the dual frequency ratio (DFR) which is defined as the difference of Ze at a frequency of Ku and Ka measured with the DPR.

In the present study, we applied a similar technique to the dual-polarization radars and estimated the relative magnitude of the attenuation in the radar propagation path. It cannot be applied to the attenuation correction, but can be useful for hydrometeor classification.

2. Method for attenuation estimate from the DFR (MAD)

Larger attenuation of the radio wave in rain, in general, occurs at higher radar frequencies. Thus, larger decreasing tendency of the measured reflectivity factor in the propagation path should appear at higher frequencies for homogeneous precipitation. The different attenuation properties can be used to estimate the specific attenuation from measurements by using the DPR (Liao, and Meneghini, 2011).

The DPR onboard the GPM core satellite operates at frequencies of Ku-band (14GHz) and Ka-band (35GHz). The dual frequency ratio (DFR) is obtained from the DPR and is the defined as,

$$DFR = Z_e(Ku:dBZ) - Z_e(Ka:dBZ). \qquad (2.1)$$

For rain of small size of raindrops, the scattering properties both at Ka and Ku-band radar are in the Rayleigh regime, which results in small values of the DFR unless attenuation is significant. For rain of large size of raindrops, the scattering properties at Ka-band radar is in the Mie regime but are still in the Rayleigh regime at Ku-band radar, which results in larger value of the DFR. For snow, on the other hand, the scattering properties are in the Mie regime both for Ka and Ku-band radar. Larger size of particles generally leads to larger values of the DFR. The DFR associated with the different scattering properties of particles between Ka and Ku-band (DFRs) is called here as 'scattering effect'.

In addition to the scattering effects, attenuation due to rain results in increases in the DFR. Attenuation due to rain is not significant for Ku-band but is significant for Ka-band. This different attenuation property enhances the DFR. For dry snow, attenuation can be usually neglected both for Ka and Ku-band radar. It should be mentioned that "dry snow" is defined here as pure ice snow which is composed of ice and air. The DFR associated with the different attenuation is related to rain rate and drop size and is called here as 'attenuation effect'. For dry snow, he DFR is determined by only the scattering effects because of almost no attenuation at both 35 and 14 GHz. While for rain, the DFR is determined by both the scattering and the attenuation effects. Total attenuation increases with total rain rate in the propagation path. The DFR due to the attenuation effects (DFRa), therefore, monotonically increase with the path integral rain rate.

A key factor for hydrometeor classification is the attenuation effects which tend to enhance the DFR and appear only in rain regime.

$$DFR = DFR_s + DFR_a, \quad \text{for rain.} \qquad (2.2)$$
$$DFR = DFR_s, \quad \text{for drysnow.}$$

We can, therefore, identify the medium as rain if we can detect the DFRa in the measured DFR (DFR_m). To detect the DFRa, we should firstly remove the DFRs in the DFR_m.

The scattering effects are basically related to the size of particles. Large values of the DFRs

arise primarily from large particles in size. The increases in the size of particles are, generally, associated with higher precipitation rate, ie. large Ze at Ku-band. The DFRs, therefore, can be expected to increase with Ze^t.

Figure 2.1 shows the relationship between the DFR (dotted line)、DFRs (solid line) and DFRa and Ze at Ku for rain. The DFRs is related Ze by power law as $DFRs=cZe^d$ for Ze>20dB. Coefficient c and d depend on precipitation type. The ratio of the DFR to Ze^d(Ku) is given by

$$Dz \equiv DFR / Ze^d = c + DFRa / Ze^d , \qquad (2.3)$$

Thus the parameter Dz is a measure of the DFRa. The difference of the attenuation between Ka and Ku-band increases with radar path length. Thus the DFRa and Dz monotonically tend to increase toward downward direction, depending on the path integrated rain rate (PIR) from the top of rain layer to the observation altitude if the DFRs is constant in the propagation path. Figure 2.2 shows the ratio of the DFR to Ze(Ku) versus the DFRa. The ratio is linearly related to the DFRa except for DFR/Ze<0.1 and b can be assumed to be 1. The scattering effects is expected to be removed by dividing DFR_m by Ze at Ku-band to some degree. For attenuating medium like intense rain, observed Dz increased with radar path length (Fig. 2.3). The path integrated Ze (Ku) (PIZ) from the top of rain layer instead of the PIR is used for abscissa. The correlation coefficient between Dz and PIZ is used to judge whether Dz increases with PIZ or not.

Figure 2.4 is a frequency histogram of the correlation coefficient in the case of rain (left) and snow (right). It is found that the correlation coefficients for most rain events are higher than 0.95. On the other hand, in the case of snow, there is no significant difference in the number of occurrences. From this, it can be considered that rain and snow can be discriminated from the appropriate threshold value of the correlation coefficient.

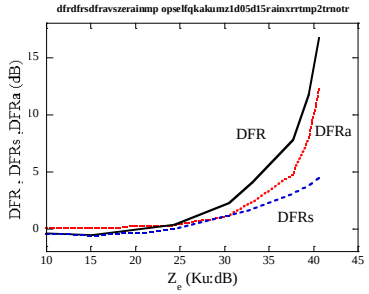

Fig.2.1 Simulated relationships between DFR,DFRs, and DFRa and Ze (left) at Ku-band for for M-P raindrop size distribution.

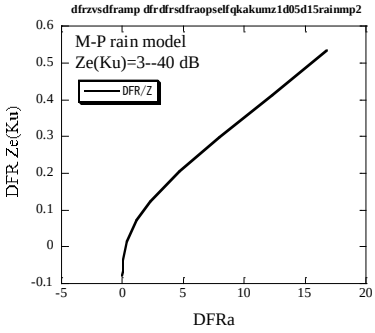

Fig.2.2 Ratio of DFR to Ze at Ku-band versus DFRa.

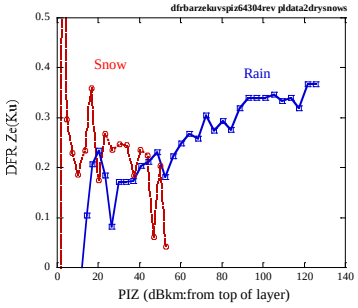

Fig.2.3 The ratio of DFRm to Zem at Ku-band versus PIZ for snow(red) and rain (black) region Zem at Ku-band (blue dots) are also plotted..

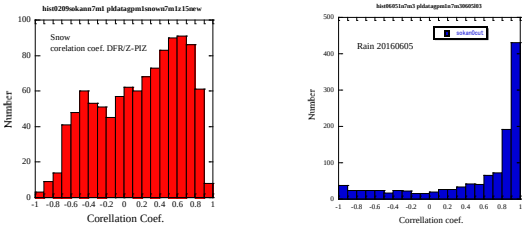

Fig.2.4 Frequency histgrams of the correlation coefficient DFR/ZE and PIZ for rain layer (each 875m thickness). for rain(left) and snow(right).

3. Method for attenuation estimate from dual polarization radar (MAP)

As mentioned earlier, the attenuation was estimated from the range variation of the DFR calculated from Ze at Ku and Ka-band which have different propagation effect, that is, different attenuation. Similar technique can be applied for a single frequency dual-polarization radar. Various polarization radar signatures, such as Ze, Zdr, Kdp, etc. have different attenuation effects. Larger attenuation effects appear in the horizontally polarized reflectivity (ZeH) than the vertically polarized (ZeV) for rain of oblate raindrops. Kdp is not affected by attenuation. We can, therefore, estimate attenuation from the range variation of parameters with different propagation effects.

One-way path-integrated attenuation at range r in linear scale (PIA) is given by

$$2PIA(r) = Z_e^t(r) - Z_e^m(r). \qquad (3.1)$$

Here, Z_e^t is 'intrinsic' (no attenuated) radar reflectivity, and Z_e^m is the measured reflectivity in linear scale. We assume that Z_e^t is related to Kdp by power law (Balakrishan and Zrnic,1990) as

$$Z_e^t(r) = aKdp^b. \qquad (3.2)$$

From (3.1) and (3.2), the path integrated attenuation is given by

$$2PIA = aKdp^b - Z_e^m(r). \qquad (3.3)$$

Devided by Kdp, (3.3) is given by,

$$Q_Z \equiv \frac{2PIA}{Kdp^b} = \frac{aKdp^b - Z_e^m}{Kdp^b}$$

$$= a - \frac{Z_e^m}{Kdp^b}. \qquad (3.4)$$

The parameter Qz is related to attenuation. The specific attenuation (Ad) of the difference of Ze can be obtained by taking derivative of (3.4) in terms of range.

$$Ad(r) = \frac{dPIA}{dr} = -kdp^b \frac{dQ_Z}{2dr} \qquad (3.5)$$

$$Ad(\Delta r) = -Kdp^b \frac{Q_Z(r+\Delta r) - Q_Z(r)}{2\Delta r} \qquad (3.6)$$

The unknown term a is removed and is the advantage of this method. In taking derivative, Kdp is assumed to be constant in the region of range Δr.

The shorter length of Δr is better for the assumption of constant Kdp. However, larger Δr is better for less noisy Kdp. The coefficient b is unknown and is taken to be 1 in this study. We intend to derive range variations of the relative value of attenuation (Fig.3.1), therefore the incorrect value of b is not serious unless large variation of b in the propagation path.

Although, scattering effect on Kdp may not negligible for X-band radar (Troomel, et al.,2013), we neglect in the simulation because exact theoretical calculation of the scattering effect is still uncertain.

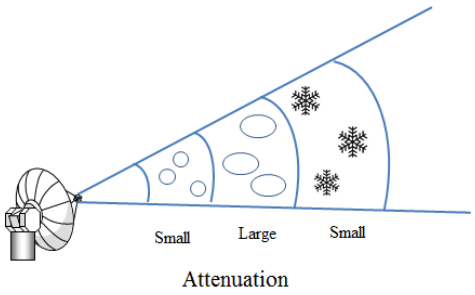

Fig.3.1 Schematic figure of the estimated range variation of the relative attenuation.

4. SIMULATIONS

We have examined the method for attenuation estimate for rain, snow and mixed-phase precipitation by using a radar simulator (GRASIA, Kobayashi et al. ,2011) which was developed for a dual polarization radar. This model is a physically-based simulator in which the scattering properties of precipitation are calculated by using the T-matrix method (Mischenko,1998). The range variations of attenuation from 0 to 20km were calculated for rain, snow, and mixed-phase precipitation and are compared with the estimated attenuation.

4.1 Hydrometeor model

Shape of raindrops is assumed to be oblate and the axis ratio changes with the drop size (Beard and Chung 1987). The size distribution of raindrops, N(D), can be expressed by an inverse exponential function, that is, Marshall-Palmer (M-P) distribution as

$$N(D) = N_0 \exp(-\Lambda D). \qquad (4.1)$$

Here, N_0 is the intercept parameter. D is the diameter of raindrops. Shape parameter Λ (mm^{-1}) is related to rain rate (R:mm/h) as $\Lambda=4.1R^{-0.21}$. Temperature of rain and snow is assumed to be 273K. The rain fall rate changes in Gaussian with radar range. The precipitation intensity is the maximum of 20 mm / h for rain at the radar range of 10 km.

Snow model used in the present study is the so called soft oblate model: shape of snow was assumed to be oblate and the refractive index of snow was calculated assuming Maxwell-Garnet (M-G) theorem for various fraction of water in snow and size of snow. The axis ratio is assumed to be constant as 0.66. The size distribution can be expressed by a modified Gamma function as,

$$N(D_m) = N_0 D_m^{\mu} \exp(-\Lambda D_m), \qquad (4.2)$$

where, D_m is major axis of snow particles. Slope parameter μ is assumed to be 3. Shape parameter Λ (mm^{-1}) is related to the mean volume equivalent diameter (D_0) and is taken to be 3.67 in the calculations. We assume snow as uniform mixture of ice, air and water and calculate the refractive index of a snow particle by using the M-G theory. Mss of snow , M can be related to the size of snow (D) and is given by,

$$M = eD^f. \qquad (4.3)$$

The coefficients e and f were given by Heymsfield et al (2004). The volume fraction of water in snow changes in Gaussian with radar range. The volume fraction of water in snow is the maximum 0.2 for rain at the radar range of 10 km. The snow fall rate is 1mm/h.

In the mixed-phase precipitation used in the present study, rain drops and ice particles coexist. The size distribution of rain was expressed by modified gamma function (μ=3, Λ=6.67) and ice particles was expressed by an inverse exponential function (Λ=0.5). The volume fraction of water in the mixed-phase precipitation increases linearly with the radar range from 0 to 1. The snow fall rate is 1 mm/h

4.2 Calculations of the attenuation

The simulations have been made for X-band radar of radar elevation angle of 0 degree. We firstly examine the assumption of the relationship between Ze^t and Kdp as shown in Eq.3.2. Figure 4.1 shows relationships of ZeH and Kdp for rain.

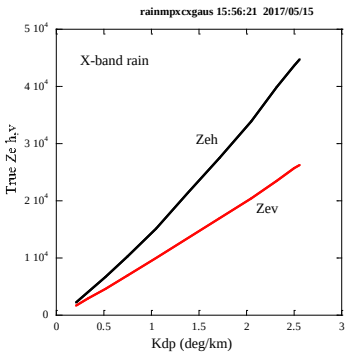

Fig.4.1 True Ze versus Kdp for rain.

Figure 4.2 shows the range variation of Q_Z and Ze for rain. Although rainfall rate is the maximum at range of 10km, the peak of the reflectivity factor Ze is around 8 km because of attenuation. The parameter Q_Z tends to monotonically increase with the range except for short range region in which small values of Kdp.

Figure 4.3 shows the range variation of relative specific attenuation of difference of ZeH (Ad) (solid line) and the theoretically calculated value (dotted line) for rain. Although there are slight differences at both ends of radar range, the overall tendencies of the range variation are in good agreement. It should be mentioned that the coefficient b is taken to be 1, therefore, the estimated attenuation is a relative value. The overestimated attenuations appear at range of smaller than 2 km and larger than 17km are associated with weak rain rate.

Figure 4.4 is same as Fig. 4.3, but for snow. The estimated attenuation (solid line) and the theoretical value (dotted line) are plotted. The both range variations are overall in good agreement. The range variation is associated with the variation of the fraction of water in snow. It is, therefore, possible to distinguish dry snow and wet snow in the propagation path.

Figure 4.5 is same as Fig. 4.3 but for mixed-phase precipitation. The estimated attenuation (solid line) and the theoretical calculated value (dotted line) are plotted. The fraction of rain amount in the mixed-phase precipitation increases with range linearly. The absorption of ice particles can be neglected and the attenuation due to scattering is also small, the attenuation of the mixed phase, therefore, increases with the fraction of rain amount. The estimated range variation is in good agreement to the theoretical range variation..

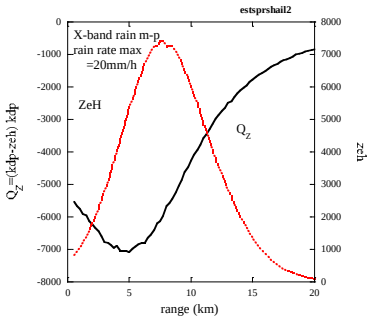

Fig.4.2 The range variation of Q_Z and Ze for rain.

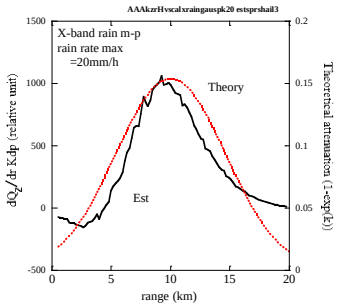

Fig.4.3 The range variation of relative specific attenuation of difference of ZeH (solid line) and the theoretical value (dotted line) for rain.

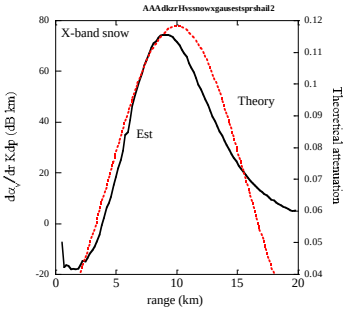

Fig.4.4 Same as Fig.4.3 but for snow.

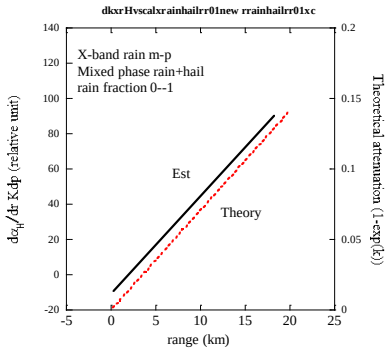

Fig.4.5 Same as Fig.4.3 but for mixed-phase precipitation.

5. OBSERVATIONS

The results of the simulations show that the range variations of the relative attenuation can be successfully obtained from Ze and Kdp. In actual observatiosn, however, Kdp is in general a noisy parameter. Therefore, whether this method can be applied to the actual observations is a subject to be proved. In this section, we will apply the method to snow measurements and examine the estimated attenuation.

There was a strong snowfall in the Kanto region from February 4th to 5th in 2014. This snowfall was observed with the X-band dual polarization radar at Funabashi. The method for attenuation estimate by using the dual polarization radar was applied to the X-band dual polarization radar and the range variations of attenuation were estimated. To verify the estimated attenuation by the MAP, we have also estimated attenuation by the dual frequency method (MAD). No GPM data was available in the snow event, we, therefore, used a ground-based C-band dual polarization radar of the Meteorological Research Institute at Tsukuba (Fig. 5.1). The C-band radar is not near the X-band radar at Funabashi but is located 41 km north-northwest of the location of the X-band radar. The observed areas measured with the C-band radar did not completely coincide with the X-band radar..

Figures 5.2 and 5.3 are radar reflectivity observed at 0 AM and 6 AM (JST) on 15th by the X and C-band dual polarization radars. The azimuthal direction of the radar beam is 195 degree. The elevation angle is 1.6 degrees for X-band radar and 0.5 degree for C-band radar. The both radars observed the same altitude at the radar range of 20km from Funabashi. The X-band radar observed precipitation at lower altitude the radar range less than 20 km and of higher altitude at longer range than 20km, because of larger elevation angles of X–band radar than the C-band radars. Although there are some differences in Ze measured with X and C-band radars at a radar range less than 10 km, the overall tendencies at a range larger than 10 km are in good agreement. It can be inferred that the altitude variation of the precipitation were small at the radar range longer than 10km.

Figure 5.4 is the range variation of the estimated attenuation by the dual frequency method (solid line) and the polarization radar method (dotted line) at 0 o'clock on 15th.
A large value indicates precipitation of large attenuation. It can be seen that there are differences between the estimated attenuation with the MAQ and MAD at a radar range less than 10 km, associated with the difference of Ze as shown in Fig. 5.2. For the radar range of larger than 10 km, the range variations of the attenuation estimated from the MAQ and MAD are in good agreement.

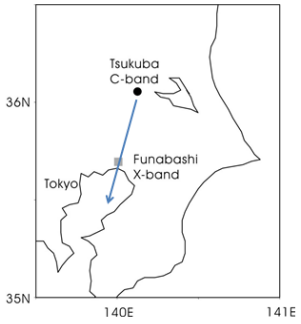

Fig.5.1 Locations of X and C-band radars.

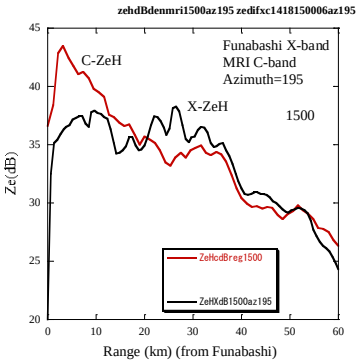

Fig.5.2 radar reflectivity observed at 0 AM (JST) on 15th by the X and C-band dual polarization radars.

The large attenuations were observed at the radar range of 30 km and 45 km and smaller attenuations were observed at the range of 38 km and 45 km. Small and large values of the ρhv were observed at large and small attenuation regions, respectively. Thus range variation of the attenuation may be related to mixed-phase.

Figure 5.5 is the same figure as Fig. 5.4 but at 6:00 PM (JST) on 15th. The estimated range variations of the attenuation are in good agreement except for the range smaller than 10 km. The large attenuations were obtained at a range from 40 to 50 km in which increases in the Zdr were observed.

6. CONCLUSIONS

Attenuation correction is critical for accurate precipitation fall-rate estimate, in particular for radars operated at higher frequencies, such as X-band. In radar measurements of precipitation, therefore, attenuation is an amount to be removed. Attenuation properties, however, depend on the type of precipitation, and therefore can be used for hydrometeor classification. Accurate attenuation amounts are not always necessary but only qualitative estimates of attenuation are enough for hydrometeor classification.

We have developed a method for estimate the range variation of the attenuation from a dual frequency radar which utilize dependence of attenuation on radar frequency. The method was applied for the GPM DPR.

In this paper, we have proposed a new method for estimate attenuation from a dual polarization radar which utilizes similar technique to the MAD. The radar reflectivity factor ZeH suffers significant attenuation. The Kdp, on the other hand, has no attenuation effects.

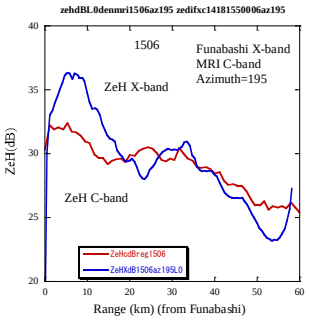

Fig.5.3 Same as Fig.5.2 but at 6.AM.

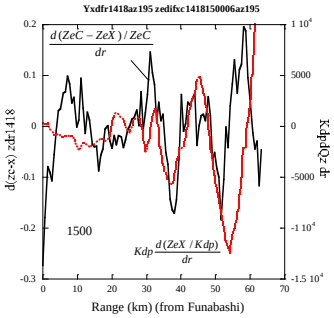

Fig.5.4 The range variation of the estimated attenuation by the dual frequency method (solid line) and the polarization radar method (dotted line) at 0 o'clock on 15th. Map of Xand C-band radars.

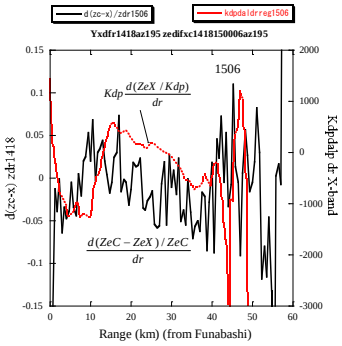

Fig.5.5 Same as Fig.5.4 but at 6 AM.

Because the amounts of attenuation should monotonically increase with radar path length, the method utilizes the range profile of Ze and Kdp instead at each radar resolution volume, for estimate relative range variation of attenuation.

We have examined the method by radar simulations for rain, snow and mixed-phase precipitation. The range variation of relative attenuation for rain in which rain fall rate changes in Gaussian with radar range, and for snow in which faction of water in snow changes in Gaussian with radar range. Simulations were also made for mixed-phase precipitation in which rain and ice particle coexists. Similar range variations of the estimated and theoretical attenuations are obtained for three cases.

We have also applied the method to X-band and C-band dual polarization radar measurements in snow. The range variations of attenuation were estimated from the MAQ for X-band radar and MAD applied for X and C-band radars. It was found that the range variations of the attenuation estimated from the both methods were in good agreement. Although this method cannot measure exact values of the specific attenuation amount, it can be expected that more accurate precipitation type discrimination becomes possible by combining with the conventional method for precipitation type discrimination.

References

Adachi, A., Takahisa Kobayashi and Hiroshi Yamauchi ,Estimation of Raindrop Size Distribution and Rainfall Rate from Polarimetric Radar Measurements at Attenuating Frequency Based on the Self-Consistency Principle, J.Meteor. Soc. Japan,

Balakrishnan N., and D. S. Zrnic, 1990, Estimation of rain and hail rates in mixed-phase precipitation, J. Atmos. Sci., 47, 565-583.

Beard, K. V., and C. Chuang, 1987: A new model for equilibrium shape of rain drops. J. Atmos. Sci., 44, 1509–1524.

Bringi, V. N., and V. Chandrasekar, N.Balakrishnan, D.S. Zrnic, 1990, An examination of propagation effects in rainfall on radar measurements at microwave frequencies, J. Atmos. Oceanic Technol., 7,829-840.2001:

Chandrasekar, et.al., 2013, Recent advamces in classification of observations from dual polarization weather radars. Atmos. Res., 119, 97-111.

Heymsfield, A.J., A. Bansemer, P. R. Field, C. Schmitt, C. Twohy, and M. R. Poellot, 2004, Effective ice particle densitys from aircraft data, *J. Atmos. Sci*., 61,982-1003

Hitschfeld, W., and J. Bordan, 1954: Errors inherent in the radar measurement of rainfall at attenuating wavelengths. *J. Meteor*. **11,** 58–67.

Iguchi, T., and R. Meneghini, 1994: Intercomparison of single-frequency methods for retrieving a vertical rain profile from airborne spaceborne radar data. *J. Atmos. Oceanic Technol.*, **11,** 1507–1516.

Kobayashi T., M. Nomura ,S. Sugimoto, F. Akimoto Furuzawa, A, Adachi, and H. Hirakuchi, 2015: Radar simulation studies for dual-frequency radar measurements of snow from space: Hydrometeor classification. Extended Abstract, 37th Conf. on Radar Meteor., Amer. Meteor. Soc., 108.

Kobayashi,T., and K. Masuda, H. Yamauchi, and A. Adachi, 2011, Physically-based Simulator for measurements of precipitation with Polarimetric and Space-borne Radars, SPIE Remote Sensing, Cheko, Praha 9/18-9/24, 2011.

Kouketsu T. et al., A,2015, A hydrometeor classification method for X-band polarimetric radar: Construction and validation focusing on solid hydrometeors under moist environments, J. Atmos. Oceanic. Technol., 32, 2052-2074.

Liao, L., and R. Meneghini, 2011, A study on the feasibility of dual-wavelength radar for identification of hydrometeor phases, *J. Appl. Meteor. Clim*, 50, 449-456

Matrosov, S., 2005: Attenuation-based estimate of rainfall rates aloft with vertically pointing Ka-band radars. J. Atmos. Oceanic Technol., 22,43-54.

Meneghini, R., and K. Nakamura, 1990: Range profiling of the rain rate by an airborne weather radar. *Remote Sens. Environ.*, **31,** 193–209.

Mischchenko, M. I.,"Capabilities and limitations of a current fortran implementation of the T-matrix method for randomly oriented ,rotationally symmetric scatters", *J. Quant. Spectrosc. Radiat. Transfer*, 60, 309-324(1998).

Thurai, M., E. Chobanyan, V.N. Bringi and B.M. Notaroš, 2015, Large raindrops against melting hail: calculation of specific differential attenuation, phase and reflectivity, ELECTRONICS LETTERS ,. 51, 1140–1142

Ryzhkov,A., M. Diederich,P. Zhang,C. Simmer,2014: Potential utilization of specific attenuation for rainfall estimation,mitigation of partial beam blockage, and radar networking, J. Atmos. Oceanic Technol., 31,599-619.

Tromel, S., M. R. Kumjian, A. V. Ryzhkov, C. Simmer, and,M. Diederich, 2013: Backscatter differential phase—Estimation and variability. J. Appl. Meteor. Climatol., 52,2529–2548